Molecular Crystals and Liquid Crystals

Publication details, including instructions for authors and subscription information:
http://www.tandfonline.com/loi/gmcl20

# Effect of Electro-Optical Memory in Liquid Crystals Doped with Carbon Nanotubes

L. Dolgov [a] , O. Yaroshchuk [a] & M. Lebovka [b]

[a] Institute of Physics, NASU, Kyiv, Ukraine

[b] Institute of Biocolloidal Chemistry, NASU, Kyiv, Ukraine

Version of record first published: 06 Jul 2012

To cite this article: L. Dolgov, O. Yaroshchuk & M. Lebovka (2008): Effect of Electro-Optical Memory in Liquid Crystals Doped with Carbon Nanotubes, Molecular Crystals and Liquid Crystals, 496:1, 212-229

To link to this article: http://dx.doi.org/10.1080/15421400802451816

*Mol. Cryst. Liq. Cryst.*, Vol. 496, pp. 212–229, 2008

ISSN: 1542-1406 print/1563-5287 online
DOI: 10.1080/15421400802451816

Taylor & Francis
Taylor & Francis Group

# Effect of Electro-Optical Memory in Liquid Crystals Doped with Carbon Nanotubes

**L. Dolgov[1], O. Yaroshchuk[1], and M. Lebovka[2]**
[1]Institute of Physics, NASU, Kyiv, Ukraine
[2]Institute of Biocolloidal Chemistry, NASU, Kyiv, Ukraine

*The electro-optical response and the microstructure of multiwalled carbon nanotubes dispersed in nematic liquid crystals with negative dielectric anisotropy are investigated. In contrast to undoped liquid crystals, the liquid crystal dispersions of carbon nanotubes are characterized by the irreversible electro-optic response or the so-called electro-optical memory effect. This effect is that the light transmittance through the sandwiched layer of the dispersion placed between two crossed polarizers considerably increases after the electric field application cycle. The state of memory persisted over months of our observation. The memory is caused by the incomplete relaxation of liquid crystal molecules from the random planar to the initial homeotropic state after the field is off. It is pointed out that the stabilization of the planar state is due to the network of small nanotube aggregates formed in the liquid crystal disturbed by electro-hydrodynamic flows. It is revealed that the efficiency of electro-optical memory depends on the network morphology and the efficiency of electro-hydrodynamic flows in a liquid crystal.*

**Keywords:** carbon nanotubes; electrohydrodynamics; electro-optical memory; liquid crystal



## 1. INTRODUCTION

Modern industry of liquid crystals (LCs) actively looks for the materials with new properties. The variety of liquid crystal display (LCD) constructions requires liquid crystal materials with the improved properties: high chemical, thermal, and photo stabilities, wide range

The investigations were carried out in the frame of the project of NASU 10-07-H "Optical, electrical, and structural peculiarities of nanodimensional heterogeneous systems carbon nanotubes–liquid crystals".

Address correspondence to L. Dolgov, Institute of Physics, NASU, 46, Nauky Pr., Kyiv 03028, Ukraine. E-mail: dolgov@iop.kiev.ua

of birefringences ($\Delta n = 0.05$–$0.2$), high dielectric anisotropy ($|\Delta\varepsilon| > 5$), high resistivity ($\rho > 10^{13}\,\text{Ohm} \cdot \text{cm}$), and wide temperature range of the liquid crystal phase ($-40^{\circ}\text{C} < T < 90^{\circ}\text{C}$) [1,2].

There are two main ways for obtaining the liquid crystals with such properties. The first way is to synthesize new compounds or to prepare new eutectic liquid crystal mixtures with the desirable features. The second way consists in mixing a liquid crystal with some non-LC dopants with the required properties.

In the 1970s, de Gennes with colleagues proposed to dope LCs by ferromagnetic nanoparticles in order to enhance its magnetic susceptibility [3]. After that, suspensions of magnetic [4,5], dielectric [6,7], metallic [8], and ferroelectric [9] nanoparticles were obtained and investigated. A small amount of these particles does not disturb essentially the liquid crystal alignment, but provides the unusual viscous, dielectric, optical, electro-, and magneto-optical properties [10].

Nanoparticle fillers can be synthesized by different ways and provided in the form of powders or colloidal dispersions. Among different fillers, a special place is occupied by carbon nanotubes (CNTs) by several reasons:

1. CNTs have different properties depending on production technology; they can be dielectric, semi-conducting, or metallic. Hence, they can differently modify properties of liquid crystals.
2. CNTs have strong anisotropy of their form. This makes them similar to molecules of calamitic LCs. In support to this fact, the dispersions of carbon nanotubes in water reveal some kind of order similar to liquid crystals [11].
3. Electron affinity of CNTs results in their effective interaction with liquid crystal molecules. Owing to this fact and a shape anisotropy, the nanotubes can be built into the liquid crystal matrix. This gives a new method to control the alignment of nanotubes [12].

So, nanotubes began to be used actively as LC fillers. This brings new means for both CNTs and LCs. The LC matrix allows one to obtain aligned ensembles of CNTs, by controlling the size, shape, and position of CNT aggregates [13,14]. The oriented layers of nanotubes can be used for the alignment of liquid crystal layers [15,16]. On the other hand, the doping of liquid crystals with nanotubes allows one to weaken the negative field effects and to decrease the driving voltage and response times for some types of LCD [17,18]. This all together proves a high interest in LC-CNT composites from scientific and application viewpoints.

In most of the previous papers devoted to the dispersions of CNTs in LCs, the accent was made on the possibility to align CNTs and to control this alignment by reorientation of the LC phase in an external field. In the present paper, we consider how another interesting property of LCs, electrohydrodynamic (EHD) convection, influences the structure of CNTs and the electro-optic response of LC-CNT composites. We show that this influence is rather strong, and it results in a new electro-optic effect called the effect of electro-optic memory.



## 2. MATERIALS AND METHODS

### 2.1. Samples

As main materials, we used two nematic LCs, EBBA and MLC6608, with negative dielectric anisotropies and nematic n-pentyl-n′-cyanobiphenyl (5CB) with positive dielectric anisotropy as an additional LC for some tests. LC EBBA (Reahim Ltd., Russia) has nematic phase in the iterval 36–77.5°C and the dielectric anisotropy $\Delta\varepsilon = -0.13$ at 40°C. Refractive indices of EBBA are $n_o = 1.535$ and $n_e = 1.785$ so that $\Delta n = 0.25$. For purification, this liquid crystal was recrystallized before the use. Nematic LC mixture MLC6608 (Merck, Germany), developed for the vertical alignment mode displays, has $\Delta\varepsilon = -4.2$ and the clearing point at 90°C. Refractive indices of MLC6608 are $n_o = 1.4748$ and $n_e = 1.5578$ ($\Delta n = 0.083$). Nematic LC 5CB (Merck, Germany) has $\Delta\varepsilon = 11.7$ and the range of the nematic mesophase 22.5–35.5°C. Two latter LCs were used without additional purification.

The multiwalled carbon nanotubes (SpecMash Ltd., Ukraine) were prepared from ethylene by the chemical vapor deposition method [19]. Typically, these CNT have an outer diameter of about 12–20 nm and the length of about tens of micrometers. The specific surface area $S$ of the tubes is 190 $m^2/g$ ($\pm$ 10%). The specific electric conductivity $\sigma$ of the powder of compressed multiwalled CNTs (at a pressure about 15 of TPa) is 10.0 S/cm along the axis of compression and appears to be significantly lower than that of graphite ($\sigma = 10^3$–$10^6$ S/cm [20]).

Liquid crystals were mixed with nanotubes by an ultrasonic mixer UZDN-2T (Russia). The mixing time was 20 min. We investigated series of samples with different contents of nanotubes: 0.004; 0.02; 0.05; 0.1; 0.5, and 1 wt % and also pure liquid crystals.

The glass substrates with transparent conductive indium tin oxide coatings and aligning polyimide layers were used for the assembling of liquid crystal cells. Liquid crystals with negative dielectric anisotropy (EBBA and MLC6608) were aligned by the layers of polyimide AL2021 (JSR, Japan) causing a homeotropic alignment. The polyimide layers

were rubbed by a fleecy cloth in order to provide a uniform planar liquid crystal alignment in the field-on state. Liquid crystal 5CB was planarly aligned on polyimide SE150 (Nissan, Japan). The cells were assembled from the polyimide substrates rubbed in the antiparallel way. The thickness of the cells was set by 16-μm glass spacers. These cells were filled capillarily with undoped liquid crystals or liquid crystals doped with nanotubes.

It was revealed that the doping of CNTs does not influence essentially the phase transition temperatures of LCs. The samples based on EBBA were investigated at a temperature of 45°C, which is remote enough from both the crystallization and clearing points. This temperature was maintained with a precision of 0.1°C by a computerized heat setting system. Measurements of MLC6608- and 5CB-based samples were carried out at room temperature.



## 2.2. Methods

For the electro-optical measurements, we used a setup designed in our laboratory. The samples were set between two crossed polarizers in such a way that the rubbing direction formed an angle of 45° with the axes of polarizers. We measured the intensity of light transmitted through the system of crossed polarizers and the sample versus the applied sinusoidal alternating voltage ($f = 2\,\text{kHz}$). The transmittance of the samples was calculated as $T = (I_{out}/I_{in})^{*}100\%$, where $I_{in}$ and $I_{out}$ are the intensities of incident and transmitted light, respectively.

The structure of CNTs and the alignment of LC in the samples were investigated by their observation in crossed polarizers, both by naked eye and in an optical polarizing microscope.

The electrical conductivity was measured for the dispersions confined between the platinum electrodes (size $d = 12\,\text{mm}$) with the interelectrode distance $h = 0.5\,\text{mm}$. Such cells were under the alternating voltage 0.1–1.2 V, which is lower than the Friedericksz transition. The frequency of the applied field was 1 kHz. So, the high frequency allowed us to avoid the polarization on electrodes and the asymmetric distribution of nanotubes in a cell [21]. It was additionally controlled that this frequency is out of the region of dielectric relaxation. The conductivity of samples was obtained by registration of inductance, capacitance, and resistance using a LCR meter 819 (Instek, 12 Hz–100 kHz). The conductivity was calculated as $\sigma = 4h/R\pi\text{d}^2$, where $R$ is the electrical resistance. The heat setting was realized by means of a thermostat 100/45 (Mechanik Pruefgeraete Medingen, Germany) and controlled with a teflon thermocouple of the K-type connected to a temperature controller Center 309 (JDC Electronic

SA, Switzerland). Each measurement was repeated at least 5 times in order to calculate the average value of the measured parameter.

## 3. RESULTS

In this section, the structuring peculiarities and physical properties of EBBA-CNT and MLC6608-CNT composites are considered separately. The results obtained for these two types of composites will be compared, and the corresponding discussion will be given in the next section.



### 3.1. EBBA-CNT Composites

#### *3.1.1. Electro-Optical Response*

In the initial state, the light transmittance $T_0$ takes minimal value. An electrical field causes the reorientation of the liquid crystal from the homeotropic to the planar state. This is accompanied with increase in the phase retardation and, thus, in the light transmittance. The phase retardation reaches values much higher than $\pi$ so that the $T(U)$ curve has oscillating character (Fig. 1). The saturation of this curve means that not only the bulk of LC but also its surface fraction are reoriented in the field. It is evident that the pristine liquid crystal, as well as LC with a small content of carbon nanotubes ($c < 0.01$ wt %), demonstrate reversible electro-optic response (Fig. 1a). A small hysteresis (1–2 V) can be explained by the field screening effect of ion charges adsorbed from the bulk of a cell on its substrate.

Dispersions with higher content of nanotubes are characterized by different forms of electro-optical curves and residual transmittances $T_m > T_0$ (Fig. 1b). The latter demonstrates the memory effect of composite samples. The memory efficiency can be characterized by the memory parameter $M$:

$$M = \frac{T_m - T_0}{T_{\max} - T_0} * 100\%, \tag{1}$$

where $T_{\max}$ is the maximum value of transmittance (Fig. 1).

The memory parameter was determined for the samples with different concentrations of nanotubes. The memory efficiency depends on the content of CNTs and the character of their aggregation in different LC hosts. Thus, the maximum value of $M$ in the EBBA-based systems is observed for $c = 0.02$–$0.05$ wt % (Fig. 2, curve *1*). At the same time, the concentration range of the efficient memory is much wider for the dispersions based on MLC6608 (Fig. 2, curve 2). In addition to

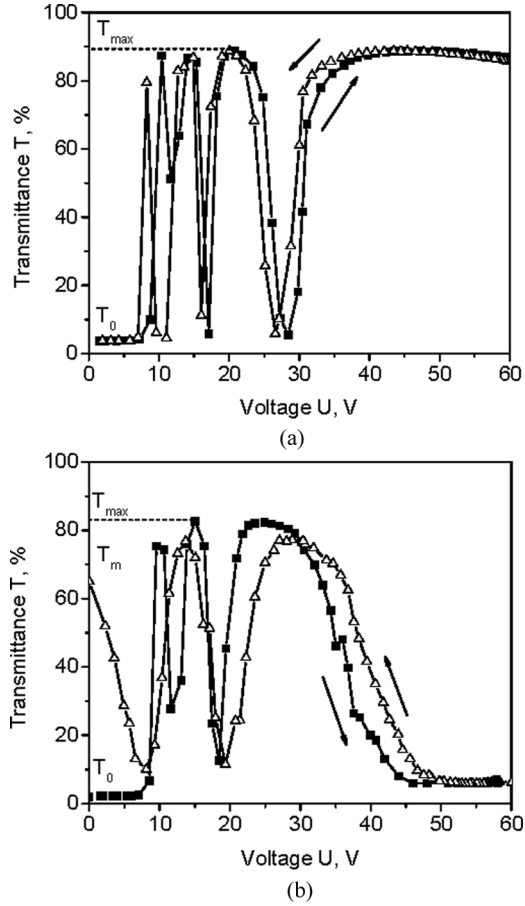


**FIGURE 1** Transmittance $T$ vs. voltage $U$ curves for the EBBA layers doped with nanotubes at different concentrations: 0 wt % (a); 0.05 wt % (b). Arrows mark the plots obtained for the increasing and decreasing voltages.

the concentration of CNTs, the memory efficiency depends on the applied voltage and the time of its action (Fig. 3). The higher the applied voltage, the shorter the time needed to achieve the memory state. However, when the voltage was lower than 10 V, the memory state was not achieved even at very long times of the voltage application.

The photographs of the cells without memory (1) and with memory (2) are presented in Figure 4. It can be seen that very small amounts of nanotubes ($c < 0.01$ wt %) do not influence the reversible switching of

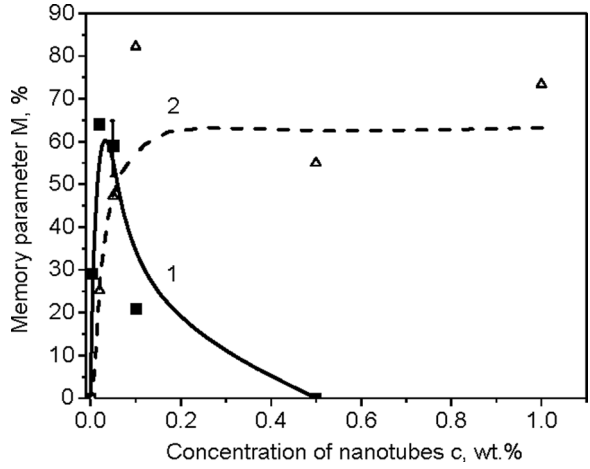


**FIGURE 2** Memory efficiency $M$ as a function of the weight concentration of nanotubes $c$ for the mixtures based on different liquid crystals: (1) EBBA-based series; 2) MLC6608-based series.

LC from the homeotropic to the planar state. However, higher concentration of nanotubes leads to the irreversible response, i.e., the appearance of the memory state. The samples capable to memory non-uniformly switch from the homeotropic to the planar state.

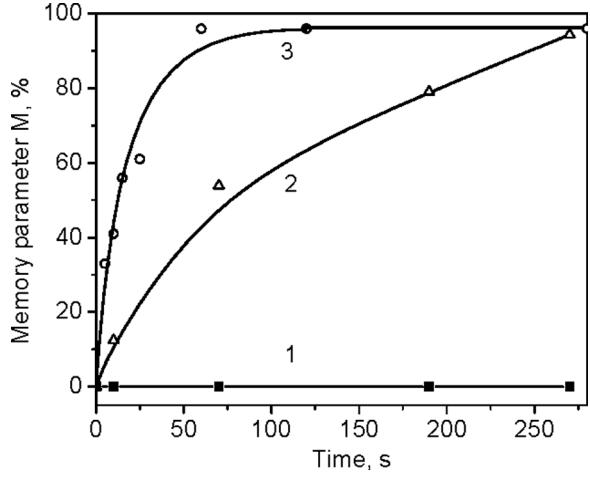


**FIGURE 3** Memory parameter $M$ as a function of the field application time for the EBBA-CNT composite ($c = 0.02$ wt %). The frequency of the applied voltage is 2 kHz; the amplitude is 10 V (1), 20 V (2), and 50 V (3).

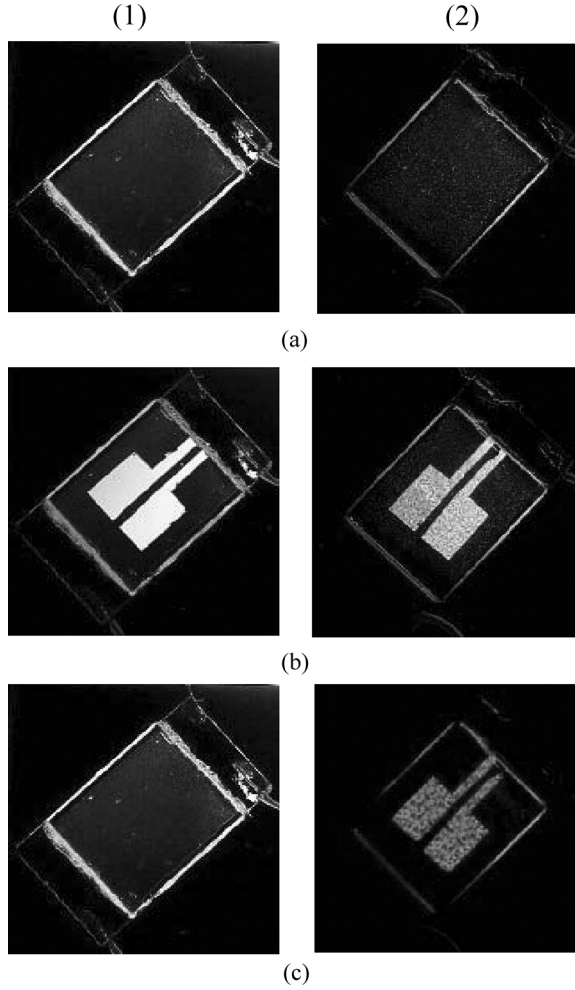


**FIGURE 4** Photographs of the cells filled with pure liquid crystal EBBA (1) and EBBA-CNT composite (2) between the crossed polarizers: (a) initial state ($U = 0$ V); (b) field-on state ($U = 60$ V, $f = 2$ kHz); (c) field-off state ($U = 0$ V). The voltage is applied to the rectangular areas of the samples.

The memory state in samples can be destroyed by application of a low-frequency voltage (10–50 Hz). The memory also vanishes after the sample cooling to the solid crystal state or heating it to the isotropic state with the following return to the mesophase.

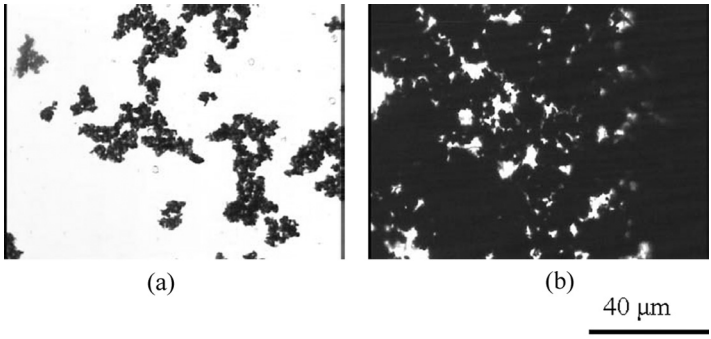


**FIGURE 5** Microphotographs of EBBA samples with different concentrations of carbon nanotubes: 0.05 wt % (a); 0.5 wt % (b).



### *3.1.2. Structure*

Similarly to other LC hosts [12,13,17,18], we observed the aggregation of CNTs in EBBA. Big aggregates are clearly visible in a polarizing microscope (Fig. 5). The size of aggregates increases up to tens and even hundreds of microns with increase in the CNT concentration. The single aggregates observed at $c < 0.02$ wt % are assembled into a continuous network, when $c > 0.5$ wt %.

The evolution of the samples' structure under the action of the high-frequency electric field ($f = 2$ kHz) depends essentially on the concentration of nanotubes. In undoped EBBA and EBBA doped with a very small amount of CNTs ($c < 0.002$ wt %), the initial homeotropic alignment state (Fig. 6a) switches to the uniform planar state (Fig. 6b) at voltages $\sim$10 V. At higher voltages, the classical electro-hydrodynamic instabilities develop in these samples. Laminar flows, revealing itself in form of the Kapustin-Williams domains, arise at $U = 80$ V [22] (Fig. 6c). As the voltage increases, the flow patterns become complicated and transform to turbulence patterns at voltages 110–120 V (Fig. 6d). The EBBA samples return to the initial homeotropic state after switching off the field (Fig. 6a).

In the samples with higher concentrations of nanotubes ($c \sim 0.02$–0.05 wt %), the development of hydrodynamic instabilities is different. At $U \sim 10$ V, liquid crystal switches from the homeotropic to the planar state (Figs. 7a, b). As the voltage increases, EHD flows appear near the aggregates of particles. The further increase in the voltage leads to the broadening of EHD areas (Fig. 7c) which overlap at $U \sim 40$ V and occupy the whole volume of the sample. At that, the Kapustin-Williams domains appear in some areas of the sample.

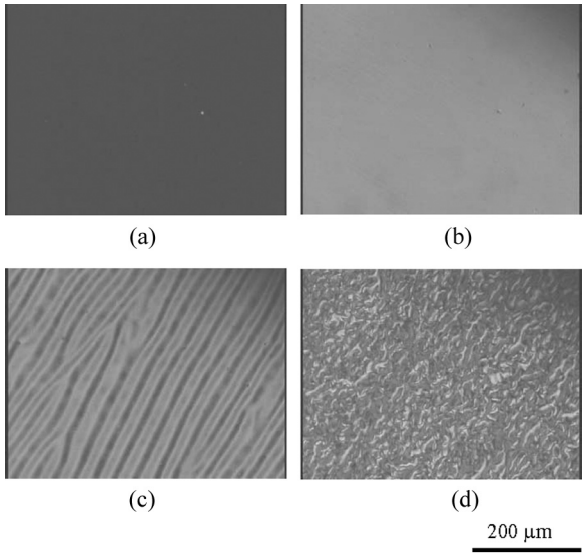


**FIGURE 6** Microphotographs of the EBBA layer subjected to alternating voltage ($f = 2$ kHz): (a) initial state ($U = 0$ V); (b) $U = 10$ V; (c) $U = 80$ V; (d) $U = 120$ V. The sample is viewed between a pair of crossed polarizers. The photographs show development of EHD flows in the layer of pure EBBA.

However, regular structure of this type was not observed. It is evident from Figure 7 that the turbulence results in the grinding of aggregates and the effective dispersion of carbon nanotubes.

Note that, in samples with a higher concentration of nanotubes ($c > 0.1$ wt %), hydrodynamic motions arose too, but they did not influence essentially the morphology of aggregates. The reason for such behavior is discussed below.

The grinding of nanotubes' aggregates and their motion in the EHD flows differ from the earlier described effects of the CNT structure reorganization related to the electrostatic and electrophoretic forces [13,14]. The effects described above were observed only in the liquid crystals with pronounced EHD instabilities.

So, the addition of carbon nanotubes to EBBA makes the electro-optical response of the liquid crystal irreversible. The samples with $c < 0.002$ wt % return to their initial homeotropic state. At the same time, the samples with $0.02 < C_{NT} < 0.5$ wt % remain in the random planar state and have the schlieren microscopic texture (Fig. 7d). This texture caused the residual transmittance $T_{\mathrm{m}}$ and the memory effect.

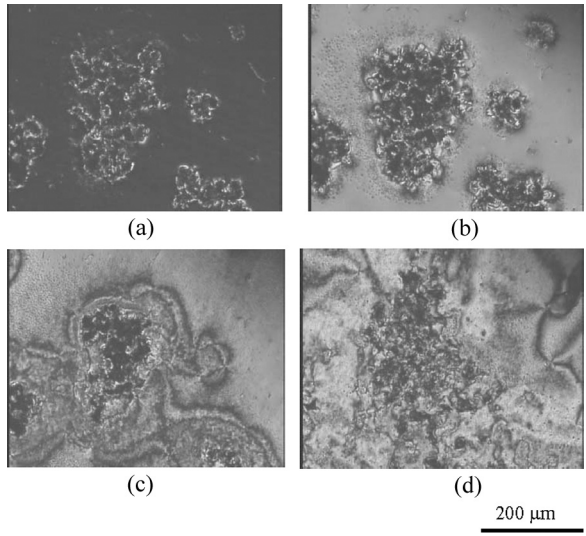


**FIGURE 7** Microphotographs of the layer of EBBA-CNT composite ($c = 0.05$ wt %) subjected to alternating voltage ($f = 2$ kHz): (a) initial state ($U = 0$ V); (b) $U = 10$ V; (c) $U = 20$ V; (d) after removing the field ($U = 0$ V). The sample is viewed between a pair of crossed polarizers. The photographs show the development of EHD flows in the layer of EBBA-CNT composite.



### *3.1.3. Conductivity of EBBA-CNT Composites*

The electrical conductivity $\sigma$ as a function of the nanotubes concentration $c$ is presented in Figure 8. The $\sigma(C_{NT})$ curve monotonically increases. One can select two areas of growth. The initial rapid growth of $\sigma$ becomes slower at concentrations 0.03–0.05 wt %. Such a change in the rate of growth is due to the achievement of the conductivity percolation threshold, when nanotubes form a three-dimensional network structure in the whole liquid crystal volume. Because the nanotubes have mainly metallic conductivity, the network formed becomes the main channel for the electric current. The charge transfer from one nanotube to another occurs admittedly by the hopping mechanism [23].

## 3.2. MLC6608-CNT Composites

### *3.2.1. Electro-Optical Response*

The $T(U)$ curves for these composites are presented in Figure 9. It is evident that these curves have a smaller number of pulsations than the corresponding curves for EBBA-CNT samples. This is caused by a smaller value of birefringence of MLC6608.

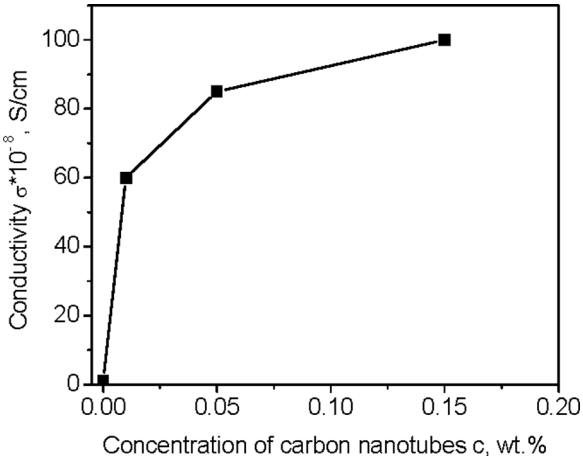


**FIGURE 8** Electrical conductivity $\sigma$ vs. the concentration of carbon nanotubes $c$ for the EBBA-based series of composites.

The dielectric anisotropy of MLC6608 is much higher than that of EBBA. This results in much smaller values of saturation voltages for MLC6608-based mixtures (~4–5 V) comparing with those for EBBA-based samples (35–40 V).

The irreversible optical response described above for EBBA-based dispersions was also observed in the dispersions based on MLC6608. The maximal memory efficiencies are similar ($M = 75$–$80\%$) for these two types of dispersions. At the same time, the concentration dependences of $M$ are essentially different. While the $M(c)$ curve for EBBA-CNT series goes through the maximum (Fig. 2, curve *1*), the corresponding curve for MLC6606-CNT series rapidly grows and saturates (at $c \sim 0.1$ wt %) (Fig. 2, curve *2*). The concentration of CNTs in our composites was less than 1 wt % to prevent the electrical breakdown. The observed differences in the $M(c)$ curves will be discussed later.

The appearance of the cells filled with MLC6608-CNT mixtures is the same as that of analogous EBBA-based samples (Fig. 4); one can see homeotropically aligned layers in the initial state and the random planar alignment during and after the removal of the field. The islets of liquid crystal in a random planar state surrounded by the CNT aggregates typically occur in the suspensions capable of electro-optic memory

### *3.2.2. Structure of MLC6608-CNT Dispersions*

Nanotubes dispersed in MLC6608 form aggregates with a broad size distribution. As in the case of EBBA-based dispersions, these

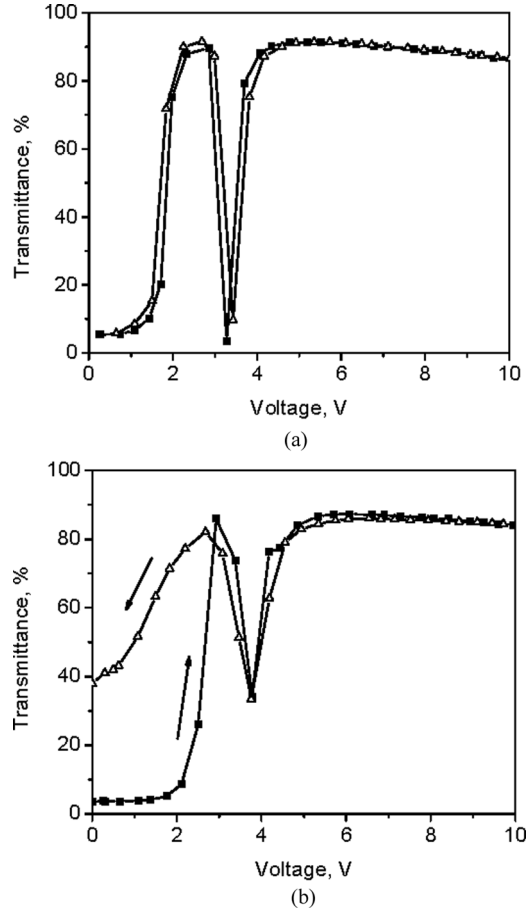


**FIGURE 9** Transmittance $T$ vs. the voltage $U$ curves for the MLC6608-CNT composites with different concentrations of nanotubes: (a) 0 wt %; (b) 0.05 wt % (b). Arrows mark the plots obtained for the increasing and decreasing voltages.

aggregates form a network at high concentrations of nanotubes. The network becomes denser with increase in the CNT content. However, at a similar CNT concentrations, the density of a network in MLC6608 composites is lower than that in the EBBA counterparts (Figs. 5 and 10).

In contrast to EBBA, MLC6608 does not reveal any hydrodynamic flows up to 100 V. It is well known [22], that the sufficient amount of ionic impurities in LC is needed for the development of hydrodynamic

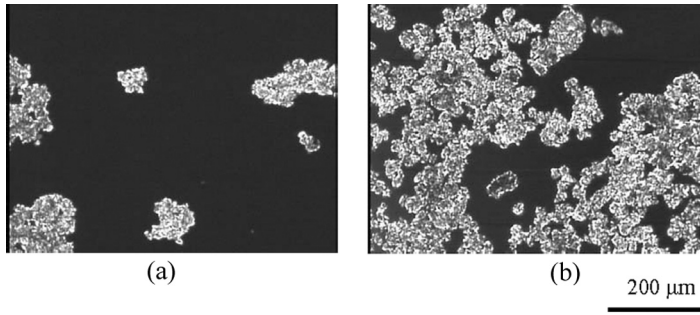


**FIGURE 10** Microphotographs of the layer of the MLC6608-CNT composite with different concentrations of carbon nanotubes: (a) 0.05 wt %; and (b) 0.5 wt % (b).



instabilities. As we have checked, the ionic conductivity of MLC6608 is one order of magnitude less than that of EBBA. This explains the difference in the efficiencies of EHD effects. The effective hydrodynamic flows in MLC6608 appear, however, after the addition of carbon nanotubes.

As in EBBA-based suspensions, two steps of the LC response to the applied field can be selected: at first, at $U = 4$–$9$ V, the Friedericksz transition occurs, and then, at higher voltages, hydrodynamic flows develop. In contrast to EBBA-based dispersions, hydrodynamics in MLC6608-based samples occurs in the form of turbulent flows without the stage of Kapustin-Williams domains. These flows begin to develop just after the Friedericksz transition in the vicinity of CNT aggregates. The areas of turbulence grow with the applied voltage and occupy the whole volume of the sample at 20–40 V. These flows result in the grinding of the aggregates of nanotubes. This dispersion process promotes the formation of a CNT network.

## 4. DISCUSSION

In this section, we consider mechanism of electro-optic memory. As noted above, the residual transmittance of memory cells is caused by the random planar alignment induced by an electric field and is remained after the field is off. It is well known that the LC alignment is imposed by interfacial layers formed between LC and the aligning substrate. Alternatively, in LC composites, the aligning surface can be distributed in the LC bulk. Taking this fact into account, one can

consider two processes leading to the stabilization of the planar LC alignment.

1. One can suppose that nanotubes modify the anchoring conditions at the aligning polyimide substrates. This may happen if CNTs are electrically polarized in the applied field and thus are adsorbed onto the substrates. If CNTs screen the alignment force of the substrate, the anchoring transition from the homeotropic to the planar alignment can occur.
2. Planar alignment state can be stabilized by a network of nanotubes which can be considered as a spatially distributed aligning surface.



In case of mechanism (1), the adsorption of nanotubes on the substrate will reduce the ionic conductivity of samples. This contradicts the fact that the ionic conductivity of the composite samples increases by about one order of magnitude after the application and subsequent removing of the electric field. Furthermore, we modeled the adsorption of CNTs in the following way. Nanotubes dispersed in methanol were spin-coated on the polyimide aligning layers. Even in case of a high surface concentration of nanotubes, the homeotropic LC alignment on polyimide was not essentially disturbed. These results show that the probability of mechanism (1) is rather low.

As for mechanism (2), the stabilization of LC structures by the particles' networks was earlier considered for LC-aerosil suspensions [6,24,25]. It was established that aerosil particles, interacting in LC by means of surface SiOH groups, form a three-dimensional network. During the LC reorientation in the electric field, this network is broken, and a new one is formed in the state of new LC alignment. The new network stabilizes a field-induced alignment after the field is off.

A similar mechanism can be responsible for the memory effect in the LC-CNT composites. According to our result, there is the percolation transition of samples' conductivity (Fig. 8) implying the formation of a CNT network. This network can stabilize a random planar alignment of LC after the field is off.

The principle of the formation of the CNT network can be, of course, different from that of the aerosil network. In contrast to aerosil particles, CNTs do not form weak hydrogen bonds, because of the absence of OH groups. The interaction forces between CNTs seem to be considerably stronger so that the simple reorientation of LC in an electric field does not crush the CNT structure. It can be crushed only at the voltages considerably higher than the Friedericksz threshold, at which EHD flows develop in the composites.

According to the results of structural studies (Figs. 5, 7, and 10), the CNT networks formed before and after the application of an electric field are different. Before switching on the field, CNTs agglomerate in big clusters forming a network structure at high concentrations ($c > 0.5$ wt %). The aggregation rate of CNTs was higher in EBBA than that in MCL6608 that can be caused by the different intensities of LC-CNT interfacial interactions, different viscosities of LCs, etc.

A much finer structure occurs after the application of an electric field. The massive CNT aggregates crushed in the electric field are assumed to form a fine network stabilizing the planar state of LC. The crushing of aggregates and the formation of the fine dispersion of CNTs was attained due to EHD flows developed in the composites. This opens a way for both the formation of a fine CNT network and, thus, the appearance of the memory effect. The decisive role of hydrodynamic flows in the formation of the fine CNT network and, thus, the memory is confirmed by other experiments. First, the memory effect was not obtained in the composites based on LC 5CB ($\Delta\varepsilon > 0$), in which EHD effects are not realized. Second, the memory effect was not observed neither in EBBA- nor in MLC6608-based composites reoriented from the homeotropic to the planar state by the magnetic field. It is well known that a magnetic field causes no hydrodynamic flows in LC.

Assuming the stabilization (memorization) of the planar state of the network of CNTs, let us finally consider the concentration dependence of the memory efficiency $M$. Comparing $M(c)$ curves (Fig. 2, curves *1* and *2*) with the concentration dependence of conductivity (Fig. 8), one can see that memory arises above the percolation threshold, i.e., when the CNT network is formed. This is in full accord with our model. The different behavior of $M(c)$ curves for EBBA- and MLC6608-based composites at high concentrations can be explained by different rates of aggregation of CNTs in these two LCs. The decay of the $M(c)$ curve for the EBBA series seems to be caused by the formation of a dense CNT network (Fig. 5b) strongly increasing the sample conductance. As we checked, the conductivity of these samples increases by more than 10 times comparing with that of undoped EBBA samples. This substantially increases the voltage drop on the samples and so decreases the actual voltage applied to the composite, even below the level, at which a memory mechanism can be launched. In addition, because of a significant current, the samples are heated up. For MLC6608-based composites, these parasitic effects are not essential.

## CONCLUSIONS

We have observed the irreversible electro-optic response of liquid crystals with $\Delta\varepsilon < 0$ doped with carbon nanotubes. It consists in the appearance of the residual transmission of aligned layers of such composites placed between two crossed polarizers in response to the application of an electric field. Such residual transmittance is due to the incomplete switching of a liquid crystal from the field-on state random planar state with a schlieren texture to the initial homeotropic state. It is shown that the random planar state is memorized due to its stabilization by the fine CNT network formed in LC in the field-on state. The important factor providing the effective dispersion of CNTs and the formation of the fine CNT network is the electrohydrodynamic convection.



## REFERENCES

[1] Yang, D.-K. & Wu, S.-T. (2006). *Fundamentals of Liquid Crystal Devices*, Chapter 6, Wiley: New York.
[2] Chigrinov, V. (1999). *Liquid Crystal Devices: Physics and Applications*, Chapter 1, Artech House: Boston, London.
[3] Brochard, F. & de Gennes, P. G. (1970). *J. Phys. (Paris)*, *31*, 691.
[4] Chen, S.-H. & Amer, N. M. (1983). *Phys. Rev. Lett.*, *51*, 2298.
[5] Buluy, O., Ouskova, E., Reznikov, Yu., Glushchenko, A., West, J., & Reshetnyak, V. (2002). *Journal of Magnetism and Magnetic Materials*, *252*, 159.
[6] Glushchenko, A. & Yaroshchuk, O. (1999). *Mol. Cryst. Liq. Cryst.*, *330*, 415.
[7] Boxtel, M., Janssen, R., Bastiaansen, C., & Broer, D. (2001). *J. Appl. Phys.*, *89*(2), 838.
[8] Shiraishi, Y., Toshima, N., Maeda, K., Yoshikawa, H., Xu, J., & Kobayashi, S. (2002). *Appl. Phys. Lett.*, *81*(15), 2845.
[9] Li, F., Buchnev, O., II Cheon, Chae., Glushchenko, A., Reshetnyak, V., Reznikov, Yu., Sluckin, T. J., & West, J. L. (2006). *Phys. Rev. Lett.*, *97*, 147801.
[10] Stark, H. (2001). *Phys. Reports*, *351*, 387.
[11] Song, W. et al. (2003). *Science*, *302*, 1363.
[12] Dierking, I., Scalia, G., Moralez, P., & LeClere, D. (2004). *Adv. Mater.*, *16*(11), 865; (2005). *J. Appl. Phys.*, *97*, 044309.
[13] Jeong, S. J., Park, K. A., Jeong, S. H., Jeong, H. J., An, K. H., Nah, C. W., Pribat, D., Lee, S. H., & Lee, Y. H. Sr., (2007). *Nanoletter*, *7*(8), 2178.
[14] Srivastava, A. K., Jeong, S. J., Lee, M.-H., Lee, S. H., Jeong, S. H., & Lee, Y. H. (2007). *J. Appl. Phys.*, *102*, 043503.
[15] Russel, M., Oh, S., LaRue, I., Zhou, O., & Samulski, E. (2006). *Thin Solid Films*, *509*, 53.
[16] Vasiliev, P. Ya. & Kamanina, N. V. (2007). *JTP Lett.*, *33*(18), 8.
[17] Lee, W., Wang, C.-Yu., & Shih, Yu.-C. (2004). *Appl. Phys. Lett.*, *85*(4), 513.
[18] Baik, In-Su., Jeon, S. Y., Lee, S. H., Park, K. A., Jeong, S. H., An, K. H., & Lee, Y. H. (2005). *Appl. Phys. Lett.*, *87*, 263110.
[19] Melezhyk, A. V., Sementsov, Yu. I., & Yanchenko, V. V. (2005). *Appl. Chem.*, *78*, 938.

[20] Weast, R. C. (1986). *Handbook of Chemistry and Physics*, CRC Press: Boca Raton, FL.
[21] Liu, L., Yang, Y., & Zhang, Y. (2004). *Physica E*, *24*, 343.
[22] Blinov, L. (1978). *Electro- and Magneto-Optics of Liquid Crystals*, Nauka: Moscow, (in Russian).
[23] Lisetski, L., Lebovka, N., Sidletskiy, O. Ts., Panikarskaya, V. D., Kasian, N. A., Kositsyn, S. S., Lisunova, M. O., & Melezhyk, O. V. (2007). *Funct. Mater.*, *14*(2), 233.
[24] Kreuzer, M., Tschudi, T., & Eidenschink, R. (1992). *Mol. Cryst. Liq. Cryst.*, *223*, 219.
[25] Glushchenko, A., Kresse, H., Reshetnyak, V., Reznikov, Yu., & Yaroshchuk, O. (1997). *Liq. Cryst.*, *23*(2), 241.